Theoretical Investigation of Azaphosphatrane Bases

Theresa L. Windus,† Michael W. Schmidt, and Mark S. Gordon*

Contribution from the Department of Chemistry, Iowa State University, Ames, Iowa 50011

Received June 14, 1994[⊗]

Abstract: A series of azaphosphatrane molecules of the form $ZP[NR(CH_2)_2]_3N$, where Z = H^+, F^+, Cl^+, CH_2, CH_3^+, NH, NH_2^+, O, or OH^+ and R = CH_3 or H, are compared with the parent base molecules with Z unoccupied. The proton affinities of the base molecules are determined and predictions of their relative base strengths are made. The dramatic change in the P−N transannular distance upon addition of Z and the nature of the P−N bond are investigated for these molecules. In contrast to the apparently weak Van der Waals transannular P−N interactions in the parent bases, the cationic species are shown to have some dative bonding. The effect of solvent (DMSO) on the acid−base relationships is estimated with the aid of a simple self-consistent reaction field model.

Introduction

In the past several years, our group has been interested in the nature of the bonding in polycyclic and cage compounds, such as bicyclobutanes, propellanes, and silatranes.[1] In this paper, we extend our interest in transannular bonding to the unique azaphosphatrane molecules synthesized by Verkade and co-workers.[2] The prototype azaphosphatrane, **1a** (top view and side view shown below), $\{P[N(CH_3)(CH_2)_2]_3N\}$ has

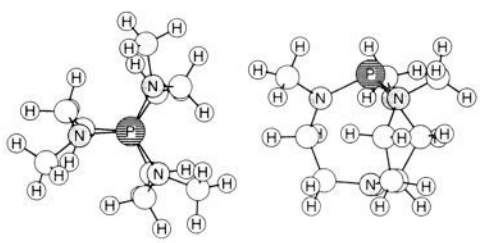

1a

been shown to be useful as a non-ionic base and as a catalyst in the synthesis of triaryl isocyanurates which are used in the synthesis of nylon-6. **1a** is a very strong base whose conjugate acid, **1b** (again shown with top and side views), has a pK_a of 27 in dimethyl sulfoxide (DMSO).

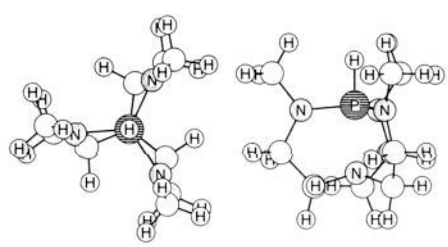

1b

This makes **1a** a stronger base than any phosphine base known. The transannular P−N distance is quite short in **1b** (1.976 Å from crystallographic data[2d]), suggesting some dative bonding, and it is very much shorter than in **1a** as found in the coordination compound *cis*-$PtCl_2$(**1a**)$_2$ (3.33 Å[2c]). The latter distance is very close to the sum of the van der Waals radii (3.35 Å).

Another interesting feature of the azaphosphatranes is the drastic change that can be made in the transannular P−N bond by varying the substituent Z on the phosphorus. X-ray structures have shown that the P−N distance can vary from about 2.0 to 3.4 Å depending on Z.[2] This large change is amazing!

In this paper, we investigate substitution effects of Z = unsubstituted, H^+, F^+, Cl^+, CH_2, CH_3^+, NH, NH_2^+, O, or OH^+ on the proton affinities of the neutrals and the nature of the transannular bond. The focus is on azaphosphatranes with either an R = methyl attached to the three nitrogens α to the phosphorus, N_e (as is usual in the experiments), or an R = hydrogen on the N_e. Using the Onsager reaction field method,[3] we also qualitatively assess the effects of solvent on the proton affinities and dipoles of the latter group of compounds.

Computational Methods

Geometries and energetics were calculated at the RHF[4]/6-31G(d)[5] level of theory. For those cases in which it was appropriate, C_3 symmetry was used in the optimization procedure. All geometries were converged so that the root mean square of the gradient was less than 0.0001 h/bohr and the maximum component of the gradient was less than 0.00003 h/bohr.

† Current address: Department of Chemistry, Northwestern University, Evanston, IL 60208-3113.

⊗ Abstract published in *Advance ACS Abstracts,* November 1, 1994.

(1) (a) Boatz, J. A.; Gordon, M. S.; Sita, L. *J. Phys. Chem.* **1990**, *94*, 5488. (b) Gordon, M. S.; Nguyen, K. A.; Carroll, M. T. *Polyhedron* **1991**, *11*, 1247. (c) Nguyen, K. A.; Carroll, M. T.; Gordon, M. S. *J. Am. Chem. Soc.* **1991**, *113*, 5998. (d) Gordon, M. S.; Carroll, M. T.; Jensen, J. H.; Davis, L. P.; Burggraf, L. W.; Guldry, R. M. *Organometallics* **1991**, *10*, 2657.

(2) (a) Lensink, C.; Xi, S. K.; Daniels, L. M.; Verkade, J. G. *J. Am. Chem. Soc.* **1989**, *111*, 3478. (b) Schmidt, H.; Lensink, C.; Xi, S. K.; Verkade, J. G. *Z. Anorg. Allg. Chem.* **1989**, *578*, 75. (c) Xi, S. K.; Schmidt, H.; Lensink, C.; Kim, S.; Wintergrass, D.; Daniels, L. M.; Jacobson, R. A.; Verkade, J. G. *Inorg. Chem.* **1990**, *29*, 2214. (d) Laramay, M. A. H.; Verkade, J. G. *J. Am. Chem. Soc.* **1990**, *112*, 9421. (e) Laramay, M. A. H.; Verkade, J. G. *Z. Anorg. Allg. Chem.* **1991**, *605*, 163. (f) Tang, J. S.; Laramay, M. A. H.; Young, V.; Ringrose, S.; Jacobson, R. A.; Verkade, J. G. *J. Am. Chem. Soc.* **1992**, *114*, 221. (g) Verkade, J. G. U.S. Patent 5,051,533, **1991**; *Chem. Abstr.* **1992**, *116*, 50379q. (h) Tang, J. S.; Verkade, J. G. *J. Am. Chem. Soc.* **1993**, *115*, 1660. (i) Tang, J. S.; Dopke, J.; Verkade, J. G. *J. Am. Chem. Soc.* **1993**, *115*, 5015. (j) Tang, J. S.; Verkade, J. G. *Angew. Chem., Int. Ed. Engl.* **1993**, *32*, 896.

(3) (a) Kirkwood, J. G. *J. Chem. Phys.* **1934**, *2*, 351. (b) Onsager, L. *J. Am. Chem. Soc.* **1936**, *58*, 1486. (c) Tapia, O.; Goscinski, O. *Mol. Phys.* **1975**, *29*, 1653. (d) Karelson, M. M.; Katritzky, A. R.; Zerner, M. C. *Int. J. Quantum Chem.* **1986**, *20*, 521. (e) Wong, M. W.; Frisch, M. J.; Wiberg, K. B. *J. Am. Chem. Soc.* **1991**, *113*, 4776. (f) Szafan, M.; Karelson, M. M.; Katritzky, A. R.; Koput, J.; Zerner, M. C. *J. Comput. Chem.* **1993**, *14*, 371.

(4) Roothaan, C. C. J. *Rev. Mod. Phys.* **1951**, *23*, 69.

0002-7863/94/1516-11449$04.50/0

Numerical second derivatives of the energy with respect to the nuclear coordinates (hessians) were only calculated for the two smallest molecules of the series $\{P[NH(CH_2)_2]_3N$ and $HP[NH(CH_2)_2]_3N^+\}$ because of the prohibitive cost of these calculations. Both of the calculated hessians were positive definite meaning that these structures are at least local minima on their respective potential energy surfaces. It should be noted here that because of the large number of degrees of freedom in these molecules, there is no assurance that the global minimum for each molecule is reached even though every effort was made to find the global minimum.

Because of the large number of basis functions (from 199 to 277), the parallel implementation of the electronic structure code GAMESS[6] was used for these calculations which were performed on the Touchstone Delta. Typical runs employed 128 or 256 nodes. Since the description of parallel GAMESS is presented elsewhere,[6,7] a discussion will not be included here.

The atoms in molecules (AIM) density analysis of Bader and coworkers[8] is used to investigate the nature of the P–N bonding in the R = H compounds. As previously reported,[1d] an extra d function needs to be added to the basis set to eliminate spurious behavior of the density. Only one additional RHF/6-31G(2d) energy calculation is performed to obtain the input and wave function needed for the AIMPAC program.[8]

Since the density analysis has been described elsewhere,[8] only a brief description of the points needed for this paper will be presented. A bond critical point is a "saddle point" in the electron density between two atoms. At this point, the hessian of the density has one positive eigenvalue along the bond (corresponding to a minimum in the electron density) and two negative eigenvalues along the axes orthogonal to the bond. A bond critical point *implies* a bond between the two atoms of interest. The other type of critical point found in this work is a ring critical point. The hessian of the density at such a point has one negative eigenvalue and two positive eigenvalues.

The Onsager reaction field[3] is used to obtain qualitative information about solvent effects. Since the azaphosphatranes are nearly spherical in nature, the spherical approximation used in this theory is well met. The dielectric constant is chosen to be that of DMSO, $\epsilon = 45.0$. The basicity experiments for **1a** + $H^+ \rightarrow$ **1b** were performed in DMSO, and it is one of the common solvents used with these molecules. The choice of cavity radius is explained below.

Results and Discussion

Figures 1 and 2 show the top view (looking down the P–N transannular "bond") of the molecules involved in this study. Full geometric information is available as supplementary material. For the remainder of this paper N_a will be used to represent the N in the transannular position (in a pseudoaxial position when a transannular bond exists) and N_e will be used to represent the N α to the phosphorus (in a pseudoequatorial position).

The top view of the R = CH_3 series is shown in Figure 1. Two different isomers were found to exist for the molecules with Z = Cl^+, NH_2^+, or OH^+. One of the isomers corresponds to a molecule with a relatively longer P–N_a bond and R = methyl groups bent down toward the cage complex (**1d**, **1i**, and **1l**). The other isomer corresponds to a molecule with a short P–N_a bond and methyl groups "popped up" into an eclipsing position with the middle CH_2 group in the side chain (**1e**, **1j**, and **1m**). For these three cations, Z = Cl^+, NH_2^+, and OH^+, the short-bond isomer lies 4.5, 6.7, and 0.9 kcal/mol higher in energy than the corresponding long-bond isomer. Note that only the three aforementioned molecules were found to have two isomers. Optimization searches for the other molecules only produced one isomer.

The cations **1b**–**1e** result from the direct attachment of X^+ to **1a**, while the other cations result from attachment of H^+ to the "axial" phosphorus substituent. By comparing the P–N_a distances in Table 1 and the molecules in Figure 1, there appears to be a correlation between a short P–N_a distance and the tendency for the methyl groups to eclipse a CH_2 (**1b**, **1c**, **1e**, **1g**, **1j**, and **1m**). All of the compounds with relatively long P–N_a distances (**1a**, **1d**, **1f**, **1h**, **1i**, **1k**, and **1l**) have the methyl group bent down toward the cage complex, rather than eclipsing the side chain CH_2 group. This type of behavior is also found in silatrane molecules.[9]

Because this trend is not found in the R = H (Figure 2) series, it is likely that this behavior is associated with the steric bulk of the methyl group. If the methyl group can move into an eclipsed position, then a relatively short P–N_a bond distance is formed. On the other hand, if the methyl group is bent toward the cage, longer P–N_a bonds are formed to relieve some of the steric strain in the system.

An exhaustive search of the potential energy surface has not been done for each molecule. However, searches for structures with eclipsing methyl groups performed in some of the neutral species (with longer P–N_a bonds) were unsuccessful.

The side chains in these molecules may also be split into two different types. The molecules with the methyls eclipsed have rather planar side chains. The lone pair of electrons on N_e occupy a very p-like orbital. The molecules with the methyl bent toward the cage have more bent side chains.

On the other hand, as can be seen in Figure 2 for R = H, the structures of the side rings are similar for all of the molecules. However, N_e does not eclipse the carbon adjacent to N_a in the cations as it does in the neutral molecules (again a flattening out of the ring around N_e occurs). This seems to be one of the largest differences between the cations and neutrals, in addition to the large changes in the P–N_a and P–Z distances.

Tables 1 and 2 show the energetics and changes in P–N_a, P–N_e, and P–Y distances associated with the series of reactions $YP[NR(CH_2)_2]_3N + X^+ \rightarrow XYP[NR(CH_2)_2]_3N^+$, where Y = unsubstituted, CH_2, NH, or O, X = H, F, or Cl, and R = CH_3 (Table 1) or H (Table 2). Note that in Table 1 when two cation isomers are present, values for both isomers are reported with the longer r(P–N_a) species reported first.

An interesting feature found in both Tables 1 and 2 is the dramatic change in the P–N_a distance. For reactions with direct attachment of X^+ onto the phosphorus atom, Δr (P–N_a) is −1.0 to −1.1 Å for R = H and −1.3 to −1.4 Å for R = CH_3. The only exception to this occurs for R = CH_3, X = Cl, in which the longer bond isomer has a Δr(P–N_a) of −0.7 Å. For compounds in which the addition of X^+ is to Y, not directly onto P, the change in the P–N_a distance is not quite as large for the R = H series (Δr(P–N_a) is −0.7 to −0.8 Å). For the R = CH_3 series, the molecules again fall into two groups: those with eclipsing methyls having a relatively large Δr(P–N_a) (−1.0 to −1.3 Å) and the others having a relatively small Δr(P–N_a) (around −0.5 Å).

In all of these molecules (including the cations), the nitrogens have negative Mulliken charges, −0.7 to −0.8 for N_a and −0.9

(5) (a) Hehre, W. J.; Ditchfield, R.; Pople, J. A. *J. Chem. Phys.* **1972**, *56*, 2257–2261. (b) Francl, M. M.; Pietro, W. J.; Hehre, W. J.; Binkley, J. S.; Gordon, M. S.; DeFrees, D. J.; Pople, J. A. *J. Chem. Phys.* **1982**, *77*, 3654–3665. (c) Gordon, M. S. *Chem. Phys. Lett.* **1980**, *76*, 163–168. (d) Ditchfield, R.; Hehre, W. J.; Pople, J. A. *J. Chem. Phys.* **1971**, *54*, 724–728. (e) Hariharan, P. C.; Pople, J. A. *Theor. Chim. Acta* **1973**, *28*, 213–222.

(6) Schmidt, M. W.; Baldridge, K. K.; Boatz, J. A.; Elbert, S. T.; Gordon, M. S.; Jensen, J. H.; Koseki, S.; Matsunaga, N.; Nguyen, K. A.; Su, S.; Windus, T. L.; Dupuis, M.; Montgomery, J. A., Jr. *J. Comp. Chem.* **1993**, *14*, 1347–1363.

(7) Windus, T. L.; Schmidt, M. W.; Gordon, M. S. *Chem. Phys. Lett.* **1993**, *216*, 375–379.

(8) (a) Bader, R. F. W.; Nguyen-Dang, T. T.; Tal, Y. *Rep. Prog. Phys.* **1981**, *44*, 893. (b) Bader, R. F. W.; Nguyen-Dang, T. T. *Adv. Quant. Chem.* **1981**, *14*, 63. (c) Bader, R. F. W. *Acc. Chem. Res.* **1985**, *18*, 9.

(9) Schmidt, M. W.; Windus, T. L.; Gordon, M. S. *J. Am. Chem. Soc.* Submitted for publication.

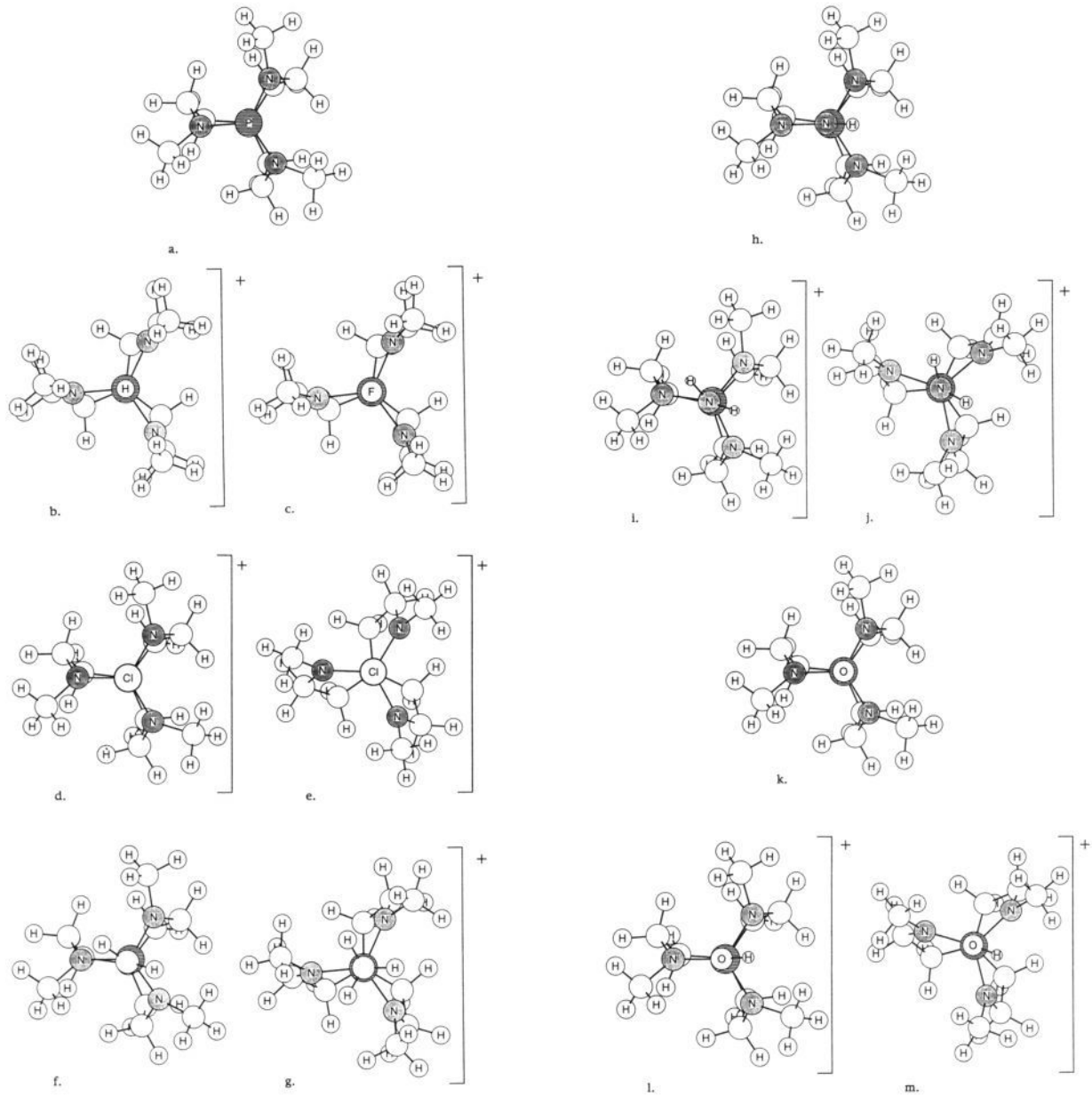

Figure 1. Top views of (a) $P[N(CH_3)(CH_2)_2]_3N$, (b) $HP[N(CH_3)(CH_2)_2]_3N^+$, (c) $FP[N(CH_3)(CH_2)_2]_3N^+$, (d, e) $ClP[N(CH_3)(CH_2)_2]_3N^+$, (f) $CH_2P[N(CH_3)(CH_2)_2]_3N$, (g) $CH_3P[N(CH_3)(CH_2)_2]_3N^+$, (h) $NHP[N(CH_3)(CH_2)_2]_3N$, (i, j) $NH_2P[N(CH_3)(CH_2)_2]_3N^+$, (k) $OP[N(CH_3)(CH_2)_2]_3N$, and (l, m) $OHP[N(CH_3)(CH_2)_2]_3N^+$.

for N_e. For those cations in which there is direct attachment of X^+ onto P, X actually assumes a negative charge (−0.1, −0.4, and −0.5 for X = H, Cl, and F, respectively). The positive charge resides mostly on P (+1.5 to +1.8). However, even for the neutrals where there is extra coordination on P, the phosphorus has a large positive charge (+1.5 to +1.6). Therefore, it appears to be the additional ligand that makes phosphorus highly positive, rather than the overall charge of the molecule. By analyzing the charges on the rest of the molecule, the positive charge of the cations is found to be spread throughout the molecule onto the carbons (which become less negative) and the hydrogens (which become more positive).

To understand the *bonding* in these species, we start by looking at the length of $P-N_a$, since this distance suggests that some bonding is present in the cationic species. Based on an RHF/6-31G(d) calculation on PH_2NH_2 (an analogue of hydrazine), a single P−N bond length is about 1.7 Å. This is 0.3−0.6 Å shorter than the $P-N_a$ distances found in the R = H cations and 0.3−1.1 Å shorter than the $P-N_a$ distances found in the R = CH_3 cations.

Also, congruent with the decrease in the $P-N_a$ bond is a lengthening of the P−Y bond. This is exactly what would be expected if some non-electrostatic bonding interaction is occurring across the transannular $P-N_a$ space. The change in the $P-N_e$ bond lengths is relatively small for these reactions. However, the trend is to decrease the $P-N_e$ bond length as the $P-N_a$ bond length decreases. Interestingly, the $P-N_e$ distance for all species is similar to the normal P−N distance in PH_2NH_2.

Figures 3a and 3b show the variation of the $P-N_a$ distance vs the N_e-P-N_e angle for R = CH_3 and H. As would be expected, the shorter $P-N_a$, the closer the N_e-P-N_e angle is to 120°. This reflects the trend of the phosphorus to become truly pentacoordinated in a trigonal bipyramidal structure as

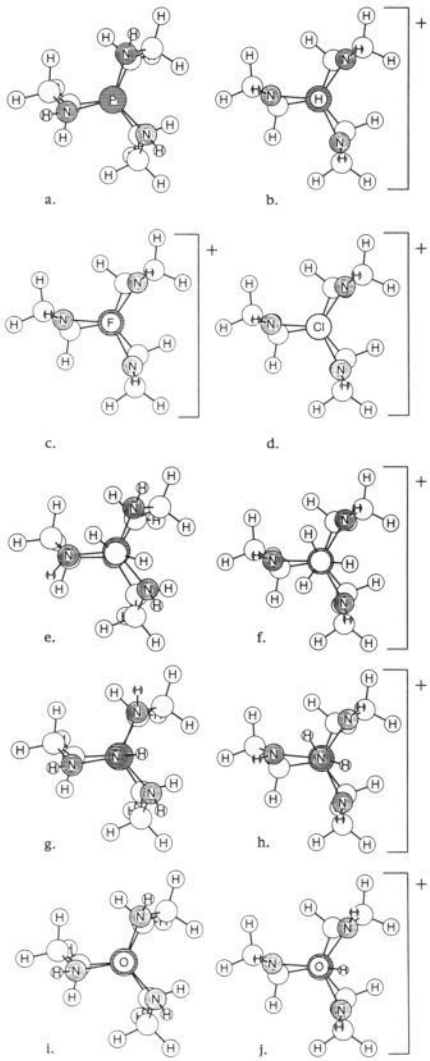

Figure 2. Top views of (a) $P[NH(CH_2)_2]_3N$, (b) $HP[NH(CH_2)_2]N^+$, (c) $FP[NH(CH_2)_2]_3N^+$, (d) $ClP[NH(CH_2)_2]_3N^+$, (e) $CH_2P[NH(CH_2)_2]_3N$, (f) $CH_3P[NH(CH_2)_2]_3N^+$, (g) $NHP[NH(CH_2)_2]_3N$, (h) $NH_2P[NH(CH_2)_2]_3N^+$, (i) $OP[NH(CH_2)_2]_3N$, and (j) $OHP[NH(CH_2)_2]_3N^+$.

$P-N_a$ decreases. The same trend is seen by Verkade and coworkers in a series of X-ray structures of $ZP[N(CH_3)(CH_2)_2]_3N$ molecules.[2]

To further explore whether or not there is a transannular bond in these molecules, we have performed an AIM analysis on each of the species involved in the R = H series. The densities at the critical points, ϱ_c, are given in Table 3. The neutral species are at the top of the table, cations are in the middle of the table, and the average ϱ_c for all of the $P-N_e$ bonds is at the bottom of the table.

Two of the neutrals (Z = CH_2 and NH) have ring critical points instead of bond critical points, suggesting that there is not a $P-N_a$ bond in these two species. The $P-N_a$ densities ϱ_c in the cations are 4−8 times larger than those in the neutrals, and in turn, the average $P-N_e$ ϱ_c is 2−3 times larger than the $P-N_a$ ϱ_c in the cations. This suggests that the cations have at least some $P-N_a$ dative bonding since the ϱ_c values associated with the cations are closer to $\varrho_c(P-N_e)$ than they are to $\varrho_c(P-N_a)$ in the neutral compounds.

To emphasize this last point, the total densities for the parent base and its conjugate acid (R = H) are plotted in Figure 4. It is clear that there is little, if any buildup of electron density between P and N_a in the base (Figure 4a), whereas there is a

Table 1. Changes in P−N Distance and Energetics for $YP[N(CH_3)(CH_2)_2]_3N + X^+ \rightarrow XYP[N(CH_3)(CH_2)_2]_3N^+$

P−Y	$X^{\pm}$	$\Delta r(P-N_a)^a$	$\Delta r(P-Y)^a$	$\Delta r(P-N_e)^{a,b}$	ΔE^c
P	H	−1.302		−0.037	−274.6
		(2.068)[d]		(1.670)[d]	
		[1.976][e]			
P	F	−1.366		−0.040	−349.7
		(2.004)[d]		(1.667)[d]	
P	Cl	−0.705		−0.079	−211.7
		(2.665)[d]		(1.628)[d]	
P	Cl	−1.371		−0.047	−207.2
		(1.998)[d]		(1.667)[d]	
$P-CH_2$	H	−1.028	+0.023	0.000	−296.6
		(2.217)[d]	(1.831)[d]	(1.684)[d]	
P−NH	H	−0.468	+0.105	−0.035	−281.8
		(2.778)[d]	(1.651)[d]	(1.638)[d]	
P−NH	H	−1.108	+0.137	+0.008	−274.1
		(2.138)[d]	(1.683)[d]	(1.681)[d]	
P−O	H	−0.529	+0.125	−0.033	−249.4
		(2.658)[d]	(1.590)[d]	(1.632)[d]	
P−O	H	−1.161	+0.152	+0.005	−248.5
		(2.027)[d]	(1.617)[d]	(1.669)[d]	

[a] Δr (Å) measures the bond length change upon addition of X^+. [b] Based on the average of the three $P-N_e$ distances. [c] ΔE (kcal/mol) measures the energy change upon addition of X^+. [d] Bond distance in angstroms for the cationic product. [e] Experimental distance from ref 2a.

Table 2. Changes in P−N Distance and Energetics for $YP[NH(CH_2)_2]_3N + X^+ \rightarrow XYP[NH(CH_2)_2]_3N^+$

P−Y	$X^{\pm}$	$\Delta r(P-N_a)^a$	$\Delta r(P-Y)^a$	$\Delta r(P-N_e)^{a,b}$	ΔE^c
P	H	−1.030		−0.059	−267.3
		(2.122)[d]		(1.656)[d]	(−258.2)[e]
		[2.078][f]			
P	F	−1.142		−0.068	−347.4
		(2.010)[d]		(1.646)[d]	
P	Cl	−1.107		−0.062	−214.8
		(2.080)[d]		(1.652)[d]	
$P-CH_2$	H	−0.766	+0.162	−0.027	−304.7
		(2.263)[d]	(1.823)[d]	(1.659)[d]	
P−NH	H	−0.730	+0.128	−0.026	−281.8
		(2.205)[d]	(1.679)[d]	(1.656)[d]	
P−O	H	−0.742	+0.148	−0.025	−252.2
		(2.094)[d]	(1.652)[d]	(1.652)[d]	

[a] Δr (Å) measures the bond length change upon addition of X^+. [b] Based on the average of the three $P-N_e$ distances. [c] ΔE (kcal/mol) measures the energy change upon addition of X^+. [d] Bond distance in angstroms for the cationic product. [e] ΔH_0 in kcal/mol, including zero point vibrational energy scaled by 0.89. [f] Experimental distance from ref 2d.

significant electron density increase in the $P-N_a$ bond region in the acid (Figure 4b). Indeed, an electron density saddle point is quite apparent in the acid.

As can be seen in Table 1 and 2, the calculated $P-N_a$ distance in $HP[NR(CH_2)_2]_3N^+$ is very close to the distance found in the crystal structures obtained by Laramay and Verkade.[2a,d] This agreement could be fortuitous, since crystal forces could make the $P-N_a$ distance shorter than would be expected in the gas phase. A measure of how important crystal forces are is provided by the energy required to decrease the $P-N_a$ distance. To explore this facet of the problem, we have performed constrained optimizations (fixing only the $P-N_a$ distance) for the neutral base and its conjugate acid at several points on either side of the equilibrium $P-N_a$ distance for R = H. Plots of the data are shown in Figure 5.

As can be seen in Figure 5, the azaphosphatrane base, **2a** in Figure 2, is rather floppy energetically with respect to changing the $P-N_a$ distance. Only about 6.5 kcal/mol is needed to compress the $P-N_a$ distance by 0.5 Å. On the other hand, to compress $P-N_a$ in the conjugate acid, **2b**, by the same amount

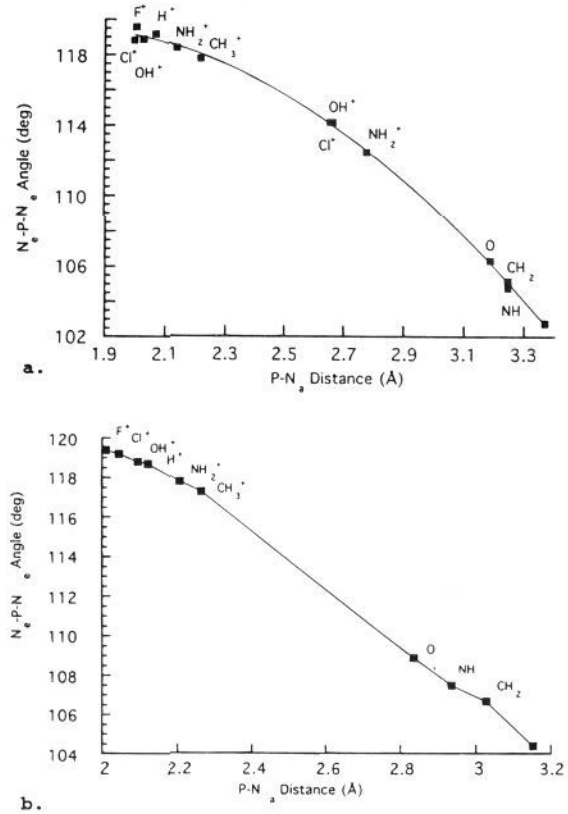

Figure 3. P−N_a versus N_e−P−N_e for (a) ZP[N(CH$_3$)(CH$_2$)$_2$]$_3$N and (b) ZP[NH(CH$_2$)$_2$]$_3$N.

Table 3. Density at the Critical Point between P and N_a for the R = H Series

P−Z	ϱ_c	index[a]
P	0.0116	b
P−CH_2	0.0137	r
P−NH	0.0154	r
P−O	0.0184	b
P−H^+	0.0756	b
P−F^+	0.0934	b
P−Cl^+	0.0883	b
P−CH_3^+	0.0585	b
P−NH_2^+	0.0648	b
P−OH^+	0.0796	b
P−N_e[b]	0.184	b

[a] The index refers to the type of critical point: b for bond and r for ring. A bond critical point has 2 negative curvatures of the electron density at the critical point, while a ring critical point has 1. [b] The average density at the bond critical points between P and N_e.

requires 33.4 kcal/mol. Of course, when the acid is compressed by 0.5 Å, the P−N_a distance is only 1.5 Å. This is shorter than our calculated P−N single bond distance of 1.7 Å in PH_2-NH_2. Nuclear repulsion is clearly playing a role in the energy increase. To compress the P−N_a distance to that of the PH_2-NH_2 distance (a decrease of 0.3 Å) requires 8 kcal/mol. This moderate change in the energy upon compression is evidence that the agreement between the calculated and experimental P−N_a distance is not fortuitous.

To lengthen the P−N_a distance requires about the same amount of energy for both the base and the acid (5.4 and 6.7 kcal/mol, respectively, for a stretch of 0.5 Å). Thus, the energy plot shown in Figure 5 for the base is fairly symmetric, while the plot for the acid is very asymmetric. This is related to both the nuclear repulsion upon compression of the acid and the weakness of the P−N_a interaction in the base.

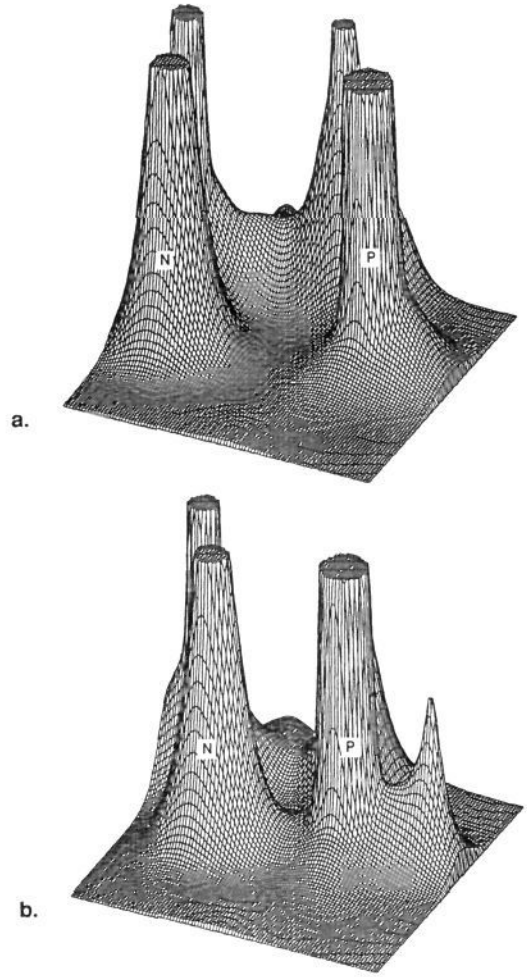

Figure 4. Total electron density plots of (a) the parent base and (b) its conjugate acid.

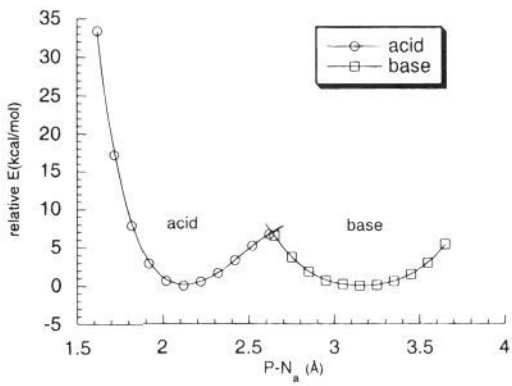

Figure 5. P−N_a distance versus relative energy for the parent base and the conjugate acid in C_3 symmetry.

By fitting a parabola to the lowest three points energetically on both plots, an estimate of the force constant associated with P−N_a can be made. This leads to estimated force constants of 0.09 h/bohr^2 for the base and 0.31 h/bohr^2 for the acid. Furthermore, from the hessian calculations for the two molecules, the internal P−N_a force constant for the base is 0.11 h/bohr^2 and that for the acid is 0.38 h/bohr^2. For comparison, the P−N_e force constant for the base is 0.30 h/bohr^2 and that for the acid is 0.45 h/bohr^2. Also, the internal force constant calculated for P−N in H_2PNH_2 is 0.32 h/bohr^2. The force constants clearly illustrate that there is much stronger P−N_a

Table 4. Changes in Energies and Dipoles for $YP[NH(CH_2)_2]_3N + H^+ \rightarrow HYP[NH(CH_2)_2]_3N^+$ in the Gas Phase and at Two Different Cavity Radii

	gas phase		4.60 Å radius		4.00 Å radius	
P–Y	ΔE^a	ΔD^b	ΔE^a	ΔD^b	ΔE^a	ΔD^b
P	267.3	−0.10 (0.64)[c]	302.6	−0.10 (0.76)[c]	307.9	−0.17 (0.76)[c]
P–CH_2	304.7	−3.72 (0.17)[c]	338.9	−4.07 (0.22)[c]	343.4	−4.54 (0.25)[c]
P–NH	281.8	−3.72 (0.28)[c]	315.7	−4.41 (0.31)[c]	320.1	−4.88 (0.33)[c]
P–O	252.2	−2.87 (2.13)[c]	285.8	−3.38 (2.44)[c]	289.9	−3.72 (2.64)[c]

[a] Change in energy in kcal/mol. [b] Change in the dipole in debyes. [c] Dipole in Debyes for the cationic species.

bonding in the acid than in the base, and that in the acid this bond is at least similar to ordinary P–N single bonds.

We now turn our attention to the energetics and, therefore, the proton affinities of these molecules, given in Tables 1 and 2.

One of the most interesting points is that the ylide system, $CH_2P[NR(CH_2)_2]_3N$, is predicted to have the largest proton affinity for both R = H (Table 2) and CH_3 (Table 1). It is, therefore, the strongest base in each of these series of molecules. (Note that this comparison is not completely "fair" since the protonation is at different atomic sites. However, the comparison is valid for the proton affinities of the following reactions: base + $H^+ \rightarrow$ acid.) Even the molecule with Y = NH is predicted to be a stronger base than the parent molecule. On the other hand, the molecule with Y = O is predicted to be a weaker base than the parent base. Our predictions have prompted further experimental investigation by the Verkade group into the ylide base.[10]

Because these bases are studied experimentally in solution, we have used the Onsager reaction field (RF) model with a dielectric constant of 45.0 (representing DMSO) to obtain a qualitative measure of the solvent effect on the proton affinities of the R = H series. Several steps are needed to estimate the solvation effects on the acid–base reactions. The first one discussed here is the choice of the cavity radius, r.

The cavity diameters for the acids and bases were chosen to be equal to the sum of the largest internuclear distance in the molecule plus the van der Waals radii of the two atoms involved. These two atoms were always hydrogen, so the van der Waals radius was taken to be 1.2 Å. The cavity radius of 4.00 Å was derived from $HP[NH(CH_2)_2]_3N^+$ and the cavity radius of 4.60 Å was derived from $CH_2P[NH(CH_2)_2]_3N$. Based on the molar volume, V_m, from crystal data[10] and the formula $r^3 = (3V_m)/(4\pi N)$ (where N is Avagodro's number), the experimental radius of the parent acid is 4.4 Å. Therefore, the calculated and experimental radii are in reasonable agreement.

The solvation data are presented in Table 4. Since, at this point in the analysis, only the cavity radius is to be determined, the energy of the H^+ is assumed to be zero. The effect of H^+ on the reaction will be discussed later in this section. Table 4 gives the changes in energy and dipole for each of the base–acid pairs for the gas phase, the solvent using a cavity radius of 4.60 Å, and the solvent using a cavity radius of 4.00 Å (all at the gas phase geometry). All dipoles are given relative to the center of mass.

The trends in the reaction energies as a function of Y are the same for all three calculations (Tables 4 and 5), so the trends in the basicities are expected to be unchanged by solvation.

(10) Private communication with Professor John Verkade.
(11) Born, M. *Z. Phys.* **1920**, *1*, 45.

Table 5. Relative Reaction Energies for $YP[NH(CH_2)_2]_3N + H^+ \rightarrow HYP[NH(CH_2)_2]_3N^+$ in the Gas Phase and at Two Different Cavity Radii

	$\Delta\Delta E^a$		
P–Y	gas phase	4.60 Å radius	4.00 Å radius
P	0.0	0.0	0.0
P–CH_2	37.4	36.3	35.5
P–NH	14.5	13.1	12.2
P–O	−15.1	−16.8	−18.0

[a] Relative energies in kcal/mol.

However, the differences in relative energies between gas phase and the two different cavity radii for a given system are as large as 3 kcal/mol. This can have a significant effect on the pK_a expected for the acid in question. A complete investigation of this requires a determination of the Gibbs free energies of the molecules which would require the prohibitively high cost calculation of hessians for all of the species.

Changes in dipole moments are also included in Table 4 since the solvent model changes the dipole moment of the molecule. Not surprisingly, molecules with the largest dipole moment are affected the most by the reaction field. The dipole moments do not change significantly for molecules with a small dipole (an example is the unsubstituted molecules) and do change quite a bit for molecules with a large dipole (an example is the molecule with Y = O).

For further exploration of these reactions, a cavity radius value of 4.3 Å (midway between the two trial values) will be used.

One of the problems with the RF model is that it does not describe bimolecular reactions well. Consider the reaction

$$A + B \rightarrow C \tag{1}$$

Ideally, to calculate the reaction energy of this system the model used should provide a size-consistent answer (i.e. the energy of A plus the energy of B should equal the energy of A and B at "infinite" separation). However, in the Onsager model the choice of r (the cavity radius) is somewhat arbitrary. This results in a model that is not size-consistent. One way to avoid this problem is to include A and B in the same calculation at "infinite" separation. However, one must then consider how to choose an appropriate value for r.

In the particular reactions considered in this work, B in reaction 1 is H^+. The only contribution to the energy from H^+ (since it has neither electrons nor a dipole) is from the Born charge term[11]

$$E_B = -{}^1/_2(1 - (1/\epsilon))Q^2/r \tag{2}$$

where ϵ = dielectric constant, Q = charge, and r = cavity radius. So, H^+ only contributes a constant factor (K) to the reaction energy once r and ϵ have been chosen.

$$\Delta E_R = E_C - E_A - E_B = E_C - E_A - K \tag{3}$$

Of course, ϵ is fixed for the entire reaction and a radius of 4.3 Å was chosen for all of the cage molecules involved. Since K is a constant for all of the reactions and since we are only interested in the trends in solution, the choice of r for H^+ is arbitrary. We have decided to use r = 4.3 Å (K = −35.29 kcal/mol), giving a model of non-interacting A + H^+ in a 4.3 Å cavity radius. As mentioned before, the choice of r is arbitrary and so only trends will be of importance.

Alternatively, consider the acid–base reaction

$$\text{base-1} + \text{acid-1} \rightarrow \text{conjugate acid-1} + \text{conjugate base-2} \tag{4}$$

using a standard basel (e.g. the parent $P[NH(CH_2)_2]_3N$). This

Table 6. Changes in P−N Distance and Energetics for $YP[NH(CH_2)_2]_3N + H^+ \rightarrow HYP[NH(CH_2)_2]_3N^+$ Using a Solvent Cavity Radius of 4.3 Å

P−Y	Δr(P−N_a)[a]	Δr(P−Y)[a]	Δr(P−N_e)[a,b]	ΔE[c]	ΔE_R[d]
P	−1.024		−0.058	−267.5	0.0
	(2.117)[e]		(1.656)[e]		
	[2.078][f]				
P−CH_2	−0.688	+0.151	−0.020	−303.3	35.8
	(2.273)[e]	(1.822)[e]	(1.664)[e]		
P−NH	−0.725	+0.120	−0.023	−279.7	12.2
	(2.205)[e]	(1.679)[e]	(1.656)[e]		
P−O	−0.694	+0.147	−0.024	−250.0	−17.5
	(2.077)[e]	(1.622)[e]	(1.653)[e]		

[a] Δr (Å) measures the bond length change upon addition of H^+. [b] Based on the average of the three P−N_e distances. [c] ΔE (kcal/mol) measures the energy change upon addition of H^+ (using a 4.3 cavity around H^+). [d] ΔE_R (kcal/mol) measures the reaction energy of $P[NH(CH_2)_2]_3N$ + acid → $HP[NH(CH_2)_2]_3N^+$ + base. [e] Bond distance in angstroms for the cationic product. [f] Experimental distance from ref 2d.

has the advantage of leaving the H^+ out of the equation. Both of the described models are used to determine the effects of the solvent reported in Table 6.

From the energetics given in Table 9 (without taking the H^+ into account), the solvent modifies the proton affinity trends by about 2−3 kcal/mol. However, these energies were calculated at the gas phase geometry. A cavity radius of 4.30 Å was used in optimizations to determine the effect of the solvent model on the geometry of the molecules. The effects of solvation on selected geometric parameters and on the energetics for the acid−base pairs (using both models) are given in Table 6.

Comparison of Table 6 with Table 2 shows that the solvation model has little effect on the geometries. In general, the trends observed in the gas phase are also observed in the solvent model. So, at least for the processes studied in this work, single point solvent energies at the gas phase geometries appear to be adequate for the determination of qualitative solvent effects for these types of molecules.

The two different models for determining basicity trends give the same results as the gas phase reaction energies. The basicity trend is Y = CH_2 > Y = NH > Y = unsubstituted > Y = O.

Conclusions

This study has explored the effects of different substituents Z in the azaphosphatrane series $ZP[NR(CH_2)_2]_3N$ where Z = unsubstituted, H^+, F^+, Cl^+, CH_2, CH_3+, NH, NH_2^+, O, or OH^+ and R = CH_3 or H. We have found four molecules (Z = CH_2 and NH for R = CH_3 and H) that are predicted to be stronger bases than the parent base (**1a** or **2a**).

Based on the P−N_a distances, Bader analyses, and constrained geometry optimizations, there is clear evidence for transannular dative bonding in the cationic species. Using the Onsager reaction field method, we have shown that the basicity trends that are found in the gas phase are also expected in DMSO.

Acknowledgment. The calculations were performed on the Touchstone Delta and on RS/6000s purchased by Iowa State University. This work was supported by a grant from the Air Force Office of Scientific Research (93−1−0105), a Department of Education GAANN fellowship to T.L.W., and assistance from the Advanced Research Projects Agency. The authors thank the Delta personnel for their help and patience and Dr. John Verkade for inspiring this work and for illuminating discussions.

Supplementary Material Available: Tables of Cartesian coordinates for the azaphosphatranes (17 pages). This material is contained in many libraries on microfiche, immediately follows this article in the microfilm version of the journal, and can be ordered from the ACS; see any current masthead page for ordering information.